# Design and Implementation of a Prototype Sunflower-Type Photovoltaic System

**Walter Naranjo Lourido, Luis Alberto Contreras Acosta, Wilver Stivenson Arana Pérez, Javier Eduardo Martínez Baquero**

*Engineering School, Faculty of Basic Sciences and Engineering, Universidad de Los Llanos, Villavicencio, Colombia (e-mail: wnaranjo@unillanos.edu.co, luis.contreras.acosta@unillanos.edu.co, wilver.arana.perez@unillanos.edu.co, jmartinez@unillanos.edu.co)*

**Abstract**: This manuscript presents the development of a functional prototype of a photovoltaic system named sunflower. It employs linear PID controllers to accurately track solar radiation. The design process initiates with the construction of a light sensor comprising three key components: transducer, conditioning, and postprocessing unit. Additionally, two PID controllers are developed to precisely adjust the position of the photovoltaic system to an orthogonal angle relative to the incident solar radiation. The results demonstrate that the sensing system effectively determines the optimal angle for solar radiation collection by the sunflower photovoltaic system. The designed controllers efficiently maximize the incidence of light energy, ensuring a stable response in the face of input changes or external disturbances. This enhancement significantly improves the prototype's accuracy, stability, and speed, even in scenarios involving multiple light energy sources.

*Keywords*: Angular positioning, PID control, Prototype sunflower, Solar radiation, Solar tracker.

## 1. INTRODUCTION

Population growth, economic development, and urbanization have led to a significant increase in energy consumption globally, which has a significant impact on the environment and the global economy. (AlAward, 2022; Bazan Navarro et al., 2023). According to data from the International Energy Agency (IEA), global electricity consumption has increased by 25% in the past decade. Coal remains the primary source, accounting for 35% of electricity generation, followed by natural gas at 24%, hydro sources at 17%, and solar power systems at 3% (International Energy Agency, n.d.).

Despite the recent surge in electricity consumption, the future of global energy consumption remains uncertain due to various external factors (Y. Zhang et al., 2022). While an increase in consumption is expected due to growing demand in developing countries and the need to meet the energy requirements of a growing population (Mauleón, 2022), it is essential to consider these uncertainties.

Numerous energy consumption challenges have been implemented worldwide to promote sustainability. These strategies include the promotion of renewable energies like wind and solar power (Ağbulut, 2022), improving energy efficiency in industries and households, stricter government policies, and raising public awareness about responsible energy consumption (Fang et al., 2023; J. Zhang et al., 2022). These efforts mitigate energy production and consumption's environmental and economic impacts.

Renewable energies play a significant role in Colombia's energy mix, with hydroelectric, wind and solar power being the primary sources (Sagastume Gutiérrez et al., 2020). Over the years, there has been a notable increase in investment and development of renewable energy projects in the country, driven by the objective of reducing dependence on fossil fuels, and promoting more sustainable energy solutions (Zapata et al., 2022).

Hydroelectric power stands as the primary source of renewable electricity generation in Colombia. Its wide availability, sustainability, reliability, and ability to meet peak energy demands have contributed to its long-standing implementation (Arias-Gaviria et al., 2019). Simultaneously, wind and solar energy sources are considered emerging sources of energy generation, showing promising potential (Pupo-Roncallo et al., 2019).

Hydroelectric energy accounts for approximately 50% of the country's electricity generation, primarily located in Tolima, Valle del Cauca, Huila, and Quindío. On the other hand, Colombia's coastal regions, such as La Guajira, Magdalena, and Sucre, possess significant wind power generation potential due to their consistent and intense winds (Gil Ruiz et al., 2022).

Colombia benefits from its favorable geographical position, receiving abundant solar radiation year-round. This resource scarcity has spurred the development of solar energy technologies (López et al., 2020).

Solar energy is experiencing remarkable growth as a renewable energy source in Colombia, contributing around 201 GWh to the country's electricity generation. Córdoba, Tolima, and Valle del Cauca are well-known for their essential role in solar energy production in Colombia. (International Energy Agency, s.f).

Unlike wind power systems, which are primarily situated along Colombia's Caribbean and Pacific coasts to maximize efficiency based on wind speed, solar power systems can be implemented across various regions in Colombia. This flexibility is due to their consistent power production in the country's coastal and inland areas (Ángel-Sanint et al., 2023).

The conversion of light energy from the sun into electrical energy is accomplished through the photovoltaic effect. This process involves the interaction of sunlight with a semiconductor material, where photons stimulate electrons, causing them to detach from their original orbits and become free electrons. These electrons then move through the semiconductor material and are captured by the electrodes at the edges, generating electrical energy (Hirst, 2012).

Consequently, the amount of electrical energy a solar panel produces depends on the quality of solar radiation it receives at any given moment. Ideally, the solar radiation should be perpendicular to the panel to maximize the conversion of light energy into electricity (Bayod-Rújula, 2019).

In recent years, the installation of rooftop solar panels has increased as a sustainable and effective solution for generating renewable energy and reducing carbon footprints in residential and commercial buildings (Ros and Sai, 2023). This installation method involves mounting photovoltaic panels on the building's roof and securing them to a racking system. Rooftop solar panels offer the advantage of utilizing available roof space and can be integrated with various roofing materials (Boxwell, 2022).

When installing a solar power system, factors such as the angle of incidence, orientation, and geographical location must be considered to optimize electricity generation. The trajectory of the sun in the sky rises from the east, moves from south to north in the northern hemisphere and from north to south in the southern hemisphere, and sets in the west (Zhong al., 2022).

Solar power systems typically installed on building roofs have a fixed tilt angle for solar panels to maximize power generation. However, large land areas are required to accommodate additional solar panels and meet the energy needs in systems with increasing energy demands. Solar panels are often installed with solar trackers to enhance energy efficiency, which can be adjusted to optimize solar radiation collection throughout the day. The tilt angle of the solar panel refers to its inclination concerning the horizontal plane (Mamodiya and Tiwari, 2021).

While single-axis solar trackers improve system efficiency during the day, their effectiveness throughout the year is limited due to a phenomenon is known as the Analemma, which prevents maximizing efficiency on all days (Hosseini Dehshiri and Firoozabadi, 2023).

The Analemma visually represents the sun's apparent path as observed from Earth. It demonstrates the sun's daily divergence in the sky compared to its expected position, caused by the Earth's axial tilt and elliptical orbit instead of a perfect circle. This phenomenon is often depicted as a figure eight shape (Saphiro, 2022).

Solar power systems are affected by the variation in solar radiation caused by the Analemma. To address this variation, two-axis solar trackers have been developed. These trackers enable the device to rotate in two directions: the tilt angle and the azimuth angle as the rotation angle (Ramful and Sowaruth, 2022).

The advantage of using a two-axis solar tracker is its higher efficiency, which allows the solar panel to be continuously and optimally oriented towards the sun, resulting in increased solar energy collection throughout the day. Furthermore, continuous sun tracking minimizes solar panel shading (Hosseini Dehshiri and Firoozabadi, 2023).

This manuscript aims to describe the procedures involved in creating a prototype solar tracker photovoltaic system with two axes of motion inspired by the behavior and appearance of Helianthus annuus, commonly known as the sunflower.

## 2. MATERIALS AND METHOD

The methodology described in Fig. 1 was followed for the project's development.

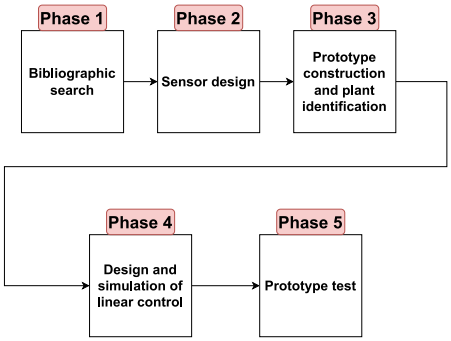


Fig. 1. Methodology by phases.

Phase 1 entails conducting extensive research, reviewing, and analyzing pertinent information to lay the groundwork for the project.

Phase 2 involves designing and constructing a sensing system to determine the sun's position in the sky accurately.

Phase 3 focuses on physically constructing the prototype to study the sensor's behavior and the plant without any control, aiming to establish its mathematical model.

Phase 4 entails designing and simulating the system to predict its behavior and evaluate its efficiency.

Phase 5 involves evaluating the prototype with linear control to assess its performance compared to the simulated behavior.

### *2.1 Sensor Transducer*

A light transducer was essential to enable the system to accurately detect the sun's position in the sky and optimize energy capture by the photocells throughout the day. This sun-tracking process aimed to enhance the efficiency of the photovoltaic system, as depicted in Fig. 2.

Various commonly used devices are available within the transducer market, such as Light Dependent Resistors (LDR), photocells, photodiodes, and phototransistors. For this research, photoresistors were chosen for their simplicity and affordability, making them suitable for measuring ambient light in low-budget applications.

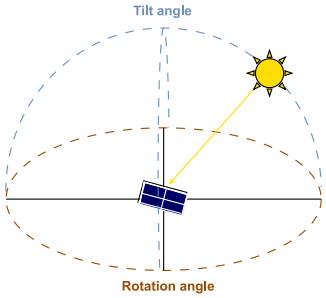


Fig. 2. Axes of the solar dome.

It is worth noting that photoresistors are passive devices that exhibit variable electrical resistance in response to the light intensity to which they are exposed. However, it is important to acknowledge that photoresistors have certain limitations. Compared to similar devices, like photodiodes or phototransistors, photoresistors has lower sensitivity and slower response speeds (Bauman, 2023). However, this does not represent an issue, due to the sun movement is slow.

Once photoresistors were chosen as transducers, we need to ensure, as a priority, a high accuracy and precision. Therefore, the selection and arrangement of photoresistors are crucial to guarantee the reliability and optimal performance of the sensing system.

The characterization process permits to identify the sensors with the least deviation between them. This process determined 20 units with similar characteristics. Various light stimuli were applied to these photoresistors, and their corresponding changes were recorded for analysis, as depicted in Fig. 3 and Fig. 4.

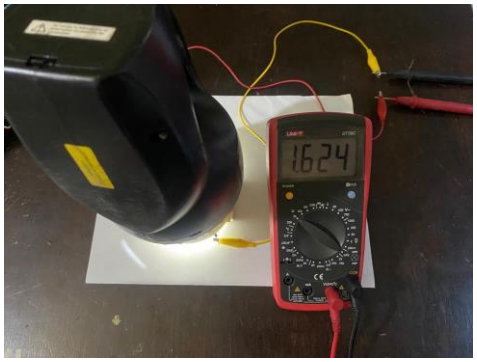


Fig. 3. The electrical resistance of an LDR under the influence of a light stimulus.

Fig. 4. LDR under the influence of a filtered light stimulus.

Table 1 illustrates the deviation results observed in five photoresistors under various light stimulations.

**Table 1. Characterization of the implemented LDR´s.**

| LED | Unfiltered light (KΩ) | Red filter light (KΩ) | Green filter light (KΩ) | Blue filter light (KΩ) | Deviation (%) |
|---|---|---|---|---|---|
| 1 | 2,5 | 3,4 | 2,7 | 2,7 | 7,91% |
| 4 | 2,4 | 3,4 | 2,6 | 2,8 | 7,50% |
| 5 | 3,0 | 3,3 | 2,8 | 2,4 | 6,12% |
| 9 | 3,0 | 3,3 | 2,6 | 2,9 | 6,61% |
| 10 | 2,4 | 3,3 | 2,7 | 2,7 | 3,70% |

*2.2 Sensor Design*

Four Light Dependent Resistors (LDRs) were strategically positioned around the base of the sensor, which features an octagonal prism shape, ensuring precise alignment for optimal capture of solar radiation. Each LDR was situated at a 90-degree angle to a plane, mimicking the cardinal points of a compass. Additionally, a tilt of -15 degrees was incorporated to facilitate radiation capture in a three-dimensional plane. A fifth LDR, positioned at the center of the base without any tilt, was responsible for capturing radiation orthogonally. All LDRs were linked to the microcontroller via a photoresistor array, following a standard configuration commonly used in light detection applications. Within this array, each LDR occupied a designated location and was interconnected in series along columns. Furthermore, each LDR was equipped with a diode for protection and individual readout purposes.

A voltage source of 5-volt was connected to each column of photoresistors to measure the voltage across each resistor. It is worth noting that as solar radiation on an LDR increases, the resistor voltage also increases, allowing for the detection and measurement of solar radiation levels.

The signal processing of the photoresistors involved two crisscrossed lines in a cross formation. One line was responsible for determining the tilt angle, while the other line determined the azimuth angle. The photoresist line was initially analyzed to calculate the angles, as illustrated in Fig. 5.

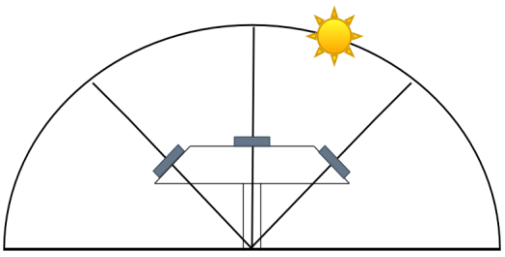

Fig. 5. LDR line diagram.

The resistors were positioned at angles of 135°, 90°, and 45° on a polar plane. Vectors with magnitudes equal to the input voltage of the microcontroller were projected at these angles.

A vector sum of these three vectors was then performed to determine the vector indicating the angle of the highest solar radiation.

Employing separate lines for the tilt and azimuth angles improves the precision of measuring the sun's direction. The system effectively identifies the angle with the highest solar radiation by utilizing the vector summation technique with vectors projected at specific angles. This signal-processing method ensures accurate and dependable measurement of the sun's direction, enhancing the overall reliability of the photoresistor-based system.

*2.3 3D modeling of the prototype*

In this section, all the necessary parts for constructing a mobile sunflower prototype were designed and manufactured in 3D. This prototype is capable of opening its petals and tracking the position of the sun.

*1) Sensor support:* The sensor base was designed in the shape of an octagonal prism to accommodate the LDRs on four opposite sides, ensuring that four LDRs were arranged at 90-degree angles to each other. A fifth LDR was positioned at the midpoint of the others to serve as an ideal radiation reference. Additionally, the base was tilted to an inclination of -15 degrees to capture radiation across a three-dimensional plane. The 3D modeling of the support is depicted in Fig. 6.

Fig. 6. AutoCad sensor support.

*2) Actuator support*: The installation comprises three actuators. Two of them track solar radiation by adjusting the tilt and azimuth angles, while the third controls the movement of the solar panels. The supports need to enable all three actuators to move concurrently. Fig. 7 illustrates the 3D model of the bracket.

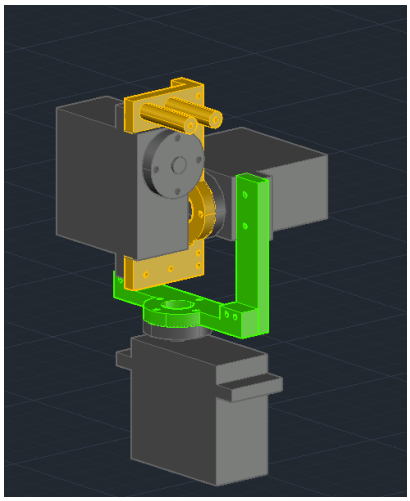

Fig. 7. AutoCad actuator support.

*3) Panel support*: The setup consists of three actuators. Two are dedicated to tracking solar radiation by adjusting tilt and azimuth angles, while the third governs the movement of the solar panels. The supports must facilitate the simultaneous movement of all three actuators. Fig. 7 depicts the 3D model of the bracket.

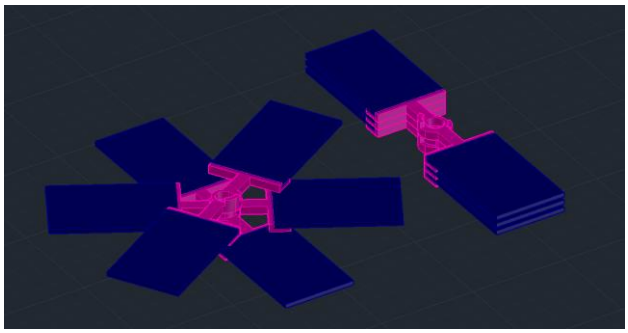

Fig. 8. AutoCad solar panels support.

Using AutoCAD, the parts for the sensing system, actuators, and solar panels were modeled. A model of the assembled parts was created to validate their design, as depicted in Fig. 9.

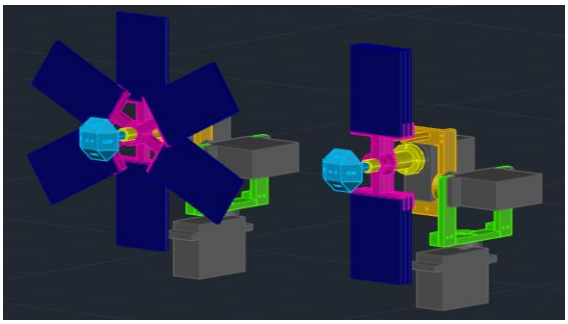

Fig. 9. 3D modeling of the prototype sunflower-type photovoltaic system.

*2.4 Design of Proportional-integral-derivative controller (PID)*

The tracking system uses two servomotors as actuators, each with a movement limit of 180°. These servomotors comprise a DC motor, a gear set, and a potentiometer functioning as position sensor. The modern microcontrollers offer libraries that converts desired angles into actuating signals. However, the utilization of these libraries has a working resolution of one degree. To achieve enhanced precision, the control signal will be manipulated across the operational frequency spectrum of the servomotor.

In this project, it used an Arduino NANO as microcontroller unit - MCU. A PWM signal, generated by the MCU using the 'writeMicroseconds' function, controls the servomotors' movements. The acceptable range of pulse width values spans from 550 microseconds to 2400 microseconds, providing a resolution of 0.097 degrees.

Design the linear control for the servomotors necessitates obtaining the mathematical model of the system. Two methodologies exist for acquiring the transfer function of a system.

The first method involves determining the transfer function by analyzing each component parameter of the system, requiring a deep understanding of the plant's physical aspects.

The second method employs system identification, which entails analyzing input and output signals to construct a mathematical model that faithfully represents the plant's behavior. For this project, the system identification toolbox for Matlab™ is utilized.

The second method was implemented, a step-type input was applied to identify each servomotor, inducing magnitude changes at specific time intervals to record the motor's behavior using the external linear potentiometer Honeywell Clarostat of 200Ohm and determine a suitable mathematical model that aligns with the observed characteristics, as depicted in Fig. 10 and Fig. 11. Both graphs exhibit similarities, particularly noticeable in their overall patterns. However, they are not identical, particularly during the initial seconds, wherein the azimuth servo demonstrates a persistent steady-state error. This discrepancy may be attributed to nonlinearities inherent in the physical model.

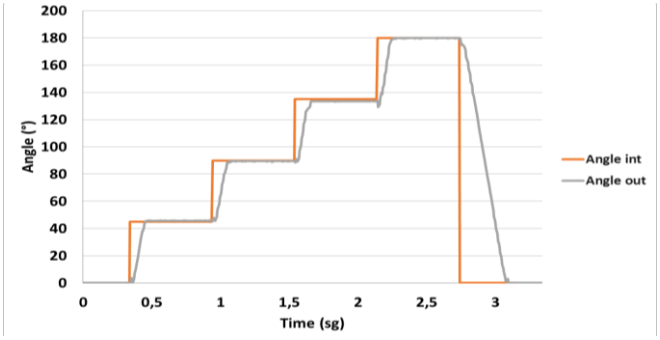


Fig. 10. Performance of the servomotor responsible for adjusting the tilt angle.

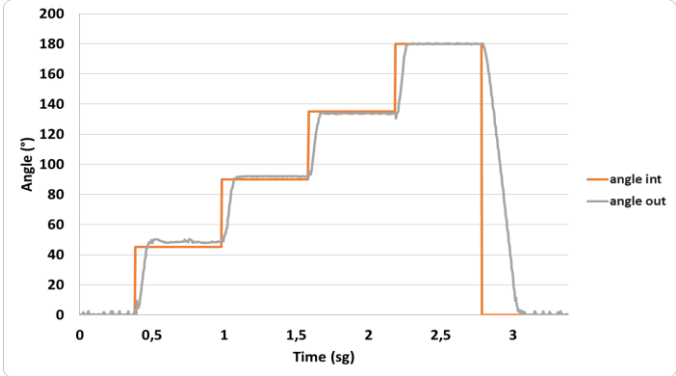


Fig. 11. Operation of the servomotor responsible for adjusting the azimuth angle.

The MATLAB system identification application starts by importing data in the time domain from both behaviors. Next, it estimates transfer function models, requiring the specification of just two parameters: the number of poles and zeros. The selected transfer function models, which best fit the data, are as follows:

$$TF_1(s) = \frac{213.3s + 47.72}{s^3 + 27.12s^2 + 215.3s + 51.41} \quad (1)$$

$$TF_2(s) = \frac{163.8s + 388.3}{s^3 + 33.53s^2 + 212.3s + 381.5} \quad (2)$$

Both transfer functions are controlling 2-axis of the sun tracking system. Transfer Function ($TF_1$), expressed in Equation (1), determines the azimuth angle displacement, while $TF_2(s)$, depicted in Equation (2), represents the transfer function governing the servomotor responsible for controlling the tilt angle displacement.

Once the model is acquired, evaluating its inherent stability becomes crucial. The configuration of the controller, such as the PID controller, can either enhance or diminish the system's stability. However, if the system is already unstable, introducing a PID controller might exacerbate the situation rather than rectify it. Assessing the stability of the uncontrolled system offers insights into its behavior and aids in selecting the most appropriate controller for the application.

Several techniques are available for assessing the inherent stability of a system without a controller, including step response analysis and Jacobian matrix analysis. In this study, the root locus stability criterion was utilized. This method entails plotting the geometric locus of the roots of the system's characteristic polynomial on the complex plane. Analyzing the root locus enables the determination of whether the system's poles lie in the left half-plane of the complex plane (indicating stability), on the imaginary axis (indicating marginal stability), or in the right half-plane (indicating instability).

Fig. 12 illustrates the zeros and poles of both transfer functions (1) and (2). Notably, the poles of the servomotor governing the azimuth angle movement are in the left half-plane, indicating robust stability for this actuator. Similarly, the poles of the servomotor regulating the tilt angle movement also reside in the left half-plane, confirming the stability of the tilt actuator. Furthermore, upon closer examination, it is evident that the poles of the tilt servomotor are nearer to the imaginary axis compared to the other servomotor, with a smaller imaginary component. As a result, these poles suggest that the servomotor controlling the tilt angle displacement will exhibit quicker dynamics and a more stable behavior than the other servomotor.

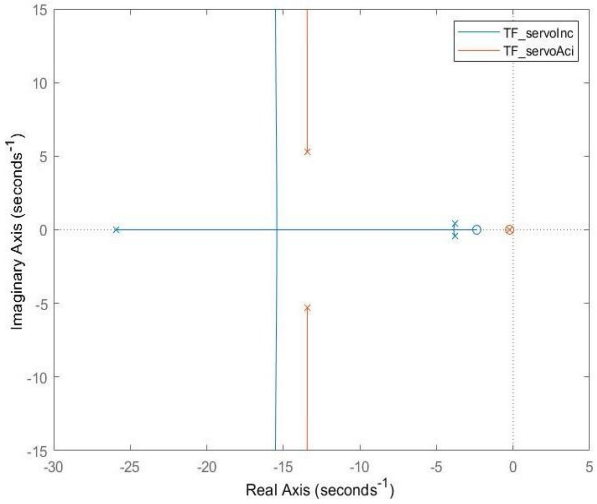


Fig. 12. Stability Assessment of Both Transfer Function.

After confirming the stability of the transfer functions, the next step was to design a linear controller. Since the controller operates through a microcontroller, converting the system from continuous to discrete time was necessary. This conversion unit for each transfer function was employed to meet the bandwidth criterion and settling time. This process allowed us to determine the appropriate sampling time interval for the conversion to discrete time. The zero-order hold method, widely used in digital control, converted the transfer functions from continuous to discrete time. Sisotool was used to adjust the PID parameters for each motor. Several parameters were established, including a maximum overshoot of less than 2% and a settling time of 2 seconds. By applying the bilinear transformation method, we can map the s-plane of the continuous-time system to the z-plane of the discrete-time system. Therefore, by employing this transformation for both transfer functions, we can derive the following equations:

$$TF_1(z) = 0.224 + 2.24\frac{T_s}{z-1} + 0.005\frac{z-1}{T_s} \quad (3)$$

$$TF_2(z) = 0.459 + 2.12\frac{T_s}{z-1} + 0.024\frac{z-1}{T_s} \quad (4)$$

The parameters of the PID controller of the servomotor in charge of the azimuth angle displacement are shown in (3) and the parameters of the PID controller of the servomotor in charge of the tilt angle displacement are shown in (4).

We have that the sampling time (T_s) is set to 0.1 to adjust the response speed.

## 3. RESULTS AND DISCUSSIONS

### *3.1. Simulations*

With the PID controller designed, we performed the corresponding simulations in each actuator using the Simulink software of MATLAB. The simulations for each servomotor are divided into two sections; the first section is simulated with Simulink Step and Ramp functions to model the behavior of the LDR corresponding to a light stimulus; the simulated LDR magnitude enters a function block that performs an algorithm similar to the microcontroller to calculate the angle orthogonal to the ideal solar incidence angle. The second section takes the reference angle to a closed-loop system with the PID controller and the plant transfer function to analyze its behavior compared to the open-loop plant transfer function.

Fig. 13 shows the input signal of the LDRs as a step input and its output at the angle calculated by the microcontroller to maximize radiation collection in the solar panels. Each step simulates the corresponding voltage input that reaches the microcontroller due to the change produced in the LDR. LDR1 and LDR3 are the LDRs positioned on the sides of the sensor, and LDR2 is the one positioned at the top, being the point where solar radiation should be greatest.

Fig. 14 shows the reference signals drawn in yellow color, the output of the plant without control drawn in orange color, and the output of the plant with linear control drawn in blue color. It can be observed that the controlled signal has a reduction of the stationary error and does not present maximum overshoot; however, its rise time is higher by a small margin.

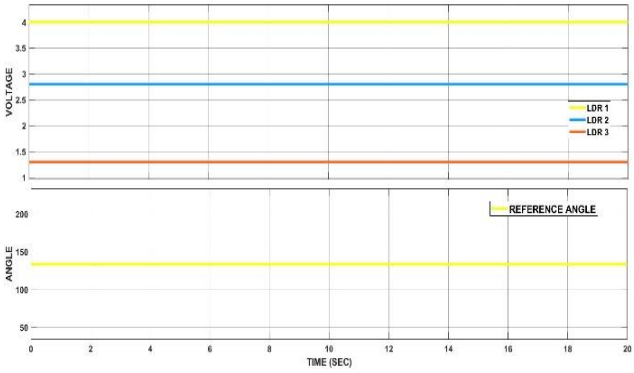


Fig. 13. Conversion from step input to a reference angle.

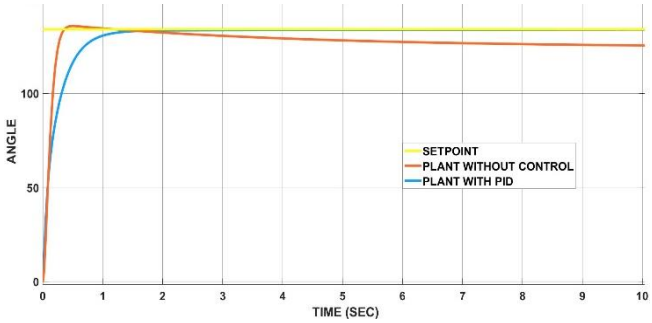


Fig. 14. Servomotor (azimuth) response to a step.

In Fig. 15, the input signal of the LDRs as input has a ramp-type behavior and its output at the angle calculated by the microcontroller to maximize the collection of radiation in the solar panels at the instant of time. With the ramp input we want to simulate a more realistic behavior of the plant's operation. Where the solar radiation affects more on an LDR located on the side of the sensor, then the plant will move so that the radiation affects more on the LDR in the center and the radiation on the LDRs on the sides is equal.

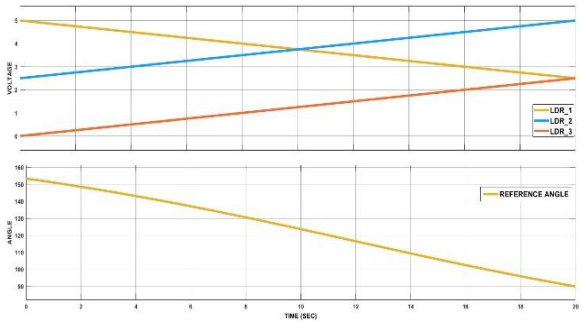


Fig. 15. Conversion of ramp type input to a reference angle.

In Fig. 16, the reference signals are depicted in blue, the plant without control in red, and the plant's output with linear control in blue. The controlled signal displays a reduction in stationary error and absence of maximum overshoot, although its rise time is prolonged. Upon comparing the behaviors of the plant, it is evident that the uncontrolled steady state error tends towards zero for step-type inputs and remains constant for ramp-type inputs, indicating that the actuators are type 1 systems.

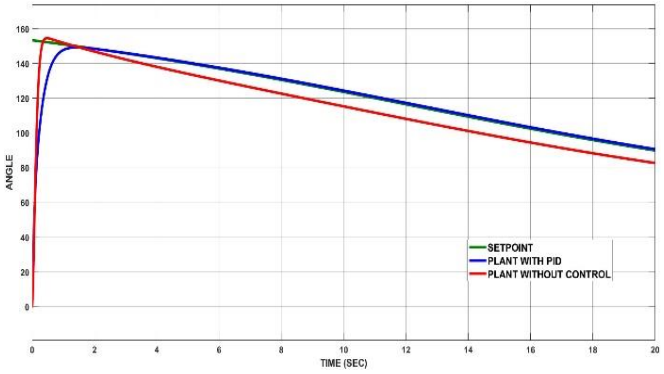


Fig. 16. Controller and servomotor in charge of the azimuth output with ramp type input.

Analysis of the simulation results for the linear PID controller designed for each actuator concludes that the controller's performance is satisfactory. Moreover, employing simulation techniques enabled a thorough and meticulous evaluation of the controller behavior across various scenarios, instilling greater confidence in its performance within the physical prototype.

*3.2. Scale prototype*

The scaled prototype of the sunflower-type photovoltaic system is built regarding the 3D modeling done, as shown in Fig. 17. The prototype meets the specifications designed in the 3D modeling to comply with the proposed behavior.

Fig. 17. Sunflower scale prototype.

During the construction process, a limitation arose because the cable connections of the elements did not allow endless rotation of the servomotor in charge of the azimuth angle. Therefore, to avoid cable winding in the prototype, the rotation of the servomotor was limited from -180° to 180°, which allowed 360° of rotation coverage and avoided cable winding at the zero-angle crossing.

To analyze the behavior of the prototype with the developed method for solar radiation tracking and the designed PID controller was decided to implement a control methodology based on logic operations with the magnitude of the LDRs; Fig. 18 shows the flow diagram of this methodology.

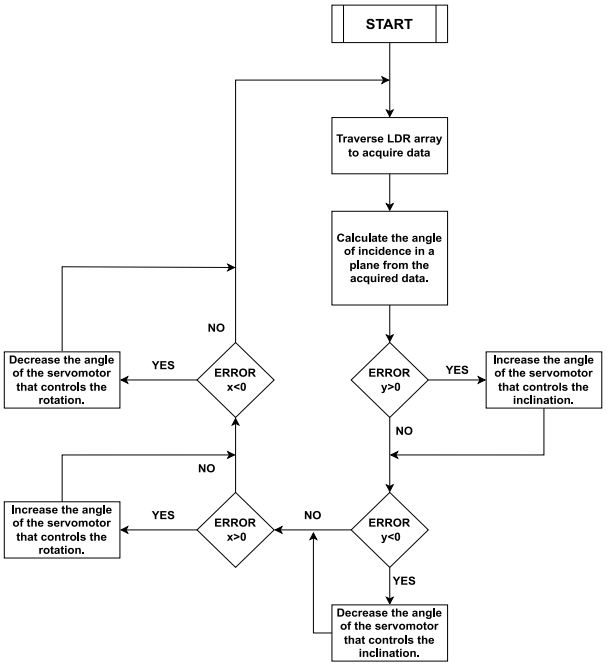


Fig. 18. Logic operation control diagram.

The implementation of control by logical operations is intended to be a reference point for comparing the performance of the developed technique with other existing methodologies in the literature. Control by logical operations emulates ON-OFF control, where the servomotors rotate in one direction until they exceed a reference point.

With the implementation of the controller by logical operations in the prototype, it could be observed that its behavior is accurate but with a high settling time. This settling time is because the servomotors are displaced a certain number of degrees in the plane before performing a new error calculation. Therefore, smaller displacement requires more iteration to reach the ideal angle, although minimal error will be obtained in the system.

The internal components of a servo motor, such as the potentiometer and other electronic components, can be viewed as angular positioning control like a proportional controller. The same logic was implemented as another prototype control methodology to compare with the developed technique.

In the proportional controller implemented in the prototype, although the actuation speed was more remarkable than when the controller by logical operations was implemented, a slight overshoot was observed for the desired angle. This overshooting phenomenon, coupled with the continuous calculation of the solar radiation angle using the LDRs, contributes to the persistent overshooting in the prototype's performance.

By implementing the PID controller in the prototype sunflower-type PV system, tracking the light radiation source with the largest incident magnitude is observed to be precise and accurate. In addition, the response speed of the prototype

is improved due to the implementation of the PID controller. Fig. 19 shows the prototype tracking a light energy source.

Fig. 19. Scale prototype following light from a flashlight.

With the prototype working correctly, angular motion information is collected over a short path from a zero point to a fixed light source with the three types of techniques explained.

In Fig. 20 and Fig. 21, the azimuth and inclination angle movements of the prototype are graphed. The blue color is with the implementation of the logic controller, the orange color is with the implementation of the proportional controller, and the gray color is with the implementation of the PID controller. It is observed that the proportional controller has a shorter establishment time than the three control techniques. However, a "variation of movement" different from the ideal is witnessed in its steady state. The PID and logic control techniques are more precise in their movement, with the PID controller having a shorter establishment time than the logical control.

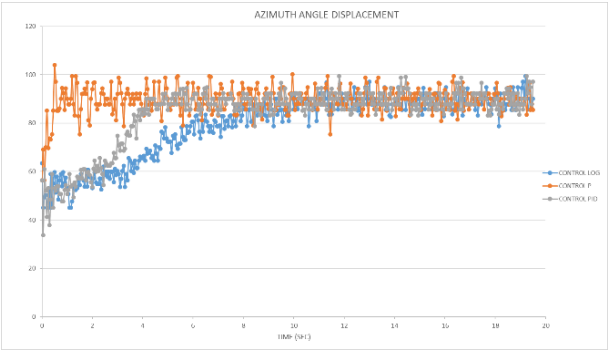


Fig. 20. Azimuth angle displacement of the scale prototype.

The sunflower-type photovoltaic system angular movement control techniques are not widely published in detail to compare the technique developed with other authors. One of the techniques that were found in the literature, is the control of the inclination angle of a sunflower-type photovoltaic system prototype through fuzzy logic, where the movement of the photocells is determined with the variation of the light intensity of two LDRs.

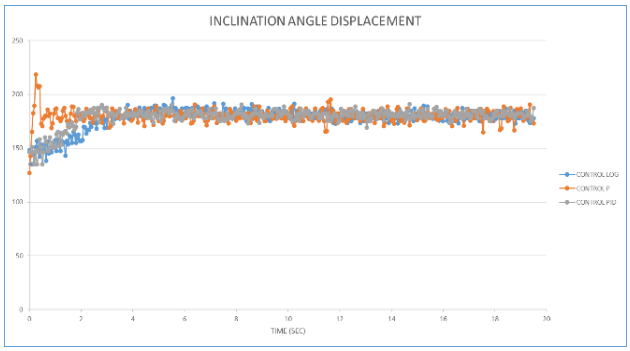


Fig. 21. Inclination angle displacement of the scale prototype.

The results presented in the work show that the fuzzy logic managed to successfully follow the path of solar radiation during the day, in spite of being a sunflower-type photovoltaic system with a single axis of movement, however it will be affected by the phenomenon of analemma (Guzman, 2020).

## 4. CONCLUSIONS

In the design of a sensing system for locating the solar radiation source, ensuring reproducibility and repeatability is paramount, especially considering the inherent variability among transducers of the same model.

Prior to the implementation of the digital controller, meticulous spatial positioning for the actuators and thorough stability analysis of the transfer function are essential. Extensive simulations with various inputs were conducted to validate the system's functionality.

Throughout the construction of the scaled prototype for the sunflower PV system, 3D modeling and printing techniques were utilized to reinforce structural stability. Following commissioning, the precise movement of the solar panels facilitated optimal capture of light radiation, even amidst multiple sources of incident light energy.

In evaluating the three control techniques for solar collection, satisfactory results were obtained. The logic controller exhibited highly accurate angular positioning with minimal error margin, albeit at a slower speed in reaching a steady-state target angle. Nevertheless, considering the dynamic changes in solar radiation affecting the photovoltaic system, the logic controller's speed of action does not compromise its viability in solar radiation tracking systems.

The proportional controller demonstrated a notable increase in actuation speed, but continuous overshoot was observed, potentially affecting the photovoltaic system's performance and durability of equipment materials.

Contrastingly, the developed PID controller showcased remarkable system action speed surpassing that of the logic operations controller, without encountering continuous overshoot observed with the proportional controller. The PID controller's rapid actuation capacity, combined with precision and stability, renders it an attractive option for highly efficient photovoltaic systems with solar tracking.

REFERENCES


Ağbulut, Ü. (2022). A novel stochastic model for very short-term wind speed forecasting in the determination of wind energy potential of a region: A case study from Turkey. *Sustainable Energy Technologies and Assessments*, 51(101853), 101853. https://doi.org/10.1016/j.seta.2021.10185.

AlAwad, M. N. J. (2022). Remarks on the world's current energy supply and demand. Journal of King Saud University - *Engineering Sciences*, 34(7), 351. https://doi.org/10.1016/j.jksues.2022.09.001

Ángel-Sanint, E., García-Orrego, S., & Ortega, S. (2023). Refining wind and solar potential maps through spatial multicriteria assessment. Case study: Colombia. *Energy for Sustainable Development: The Journal of the International Energy Initiative,* 73, 152–164. https://doi.org/10.1016/j.esd.2023.01.019

Arias-Gaviria, J., Carvajal-Quintero, S. X., & Arango-Aramburo, S. (2019). Understanding dynamics and policy for renewable energy diffusion in Colombia. *Renewable Energy*, 139, 1111–1119. https://doi.org/10.1016/j.renene.2019.02.138

Baumann, P. (2023). Optical Sensors. In Selected Sensor Circuits (pp. 43–101). *Springer Fachmedien Wiesbaden*.

Bavafa-Toosi, Y. (2017). Root locus. In *Introduction to Linear Control System*s (pp. 351–441). Elsevier.

Bayod-Rújula, A. A. (2019). Solar photovoltaics (PV). In *Solar Hydrogen Production* (pp. 237–295). Elsevier.

Bazán Navarro, C. E., Álvarez-Quiroz, V. J., Sampi, J., & Arana Sánchez, A. A. (2023). Does economic growth promote electric power consumption? Implications for electricity conservation, expansive, and security policies. *Electricity Journal*, 36(1), 107235. https://doi.org/10.1016/j.tej.2023.107235

Boxwell, M. (2022). Solar Electricity Handbook - 2022 Edition: A simple, practical guide to solar energy: how to design and install photovoltaic solar electric systems. *Greenstream Publishing*.

El Hammoumi, A., Chtita, S., Motahhir, S., & El Ghzizal, A. (2022). Solar PV energy: From material to use, and the most commonly used techniques to maximize the power output of PV systems: A focus on solar trackers and floating solar panels. *Energy Reports*, 8, 11992–12010. https://doi.org/10.1016/j.egyr.2022.09.054

Fang, G., Chen, G., Yang, K., Yin, W., & Tian, L. (2023). Can green tax policy promote China's energy transformation? A nonlinear analysis from production and consumption perspectives. *Energy* (Oxford, England), 269(126818), 126818. https://doi.org/10.1016/j.energy.2023.126818

Guzmán, S. F. P. (2020). Desarrollo de un prototipo a escala de un sistema fotovoltaico portátil autónomo tipo smart flower. Universidad De Pamplona. *http://repositoriodspace.unipamplona.edu.co/jspui/bitstream/20.500.12744/5356/1/Pombo_2020_TG.pdf*

Gil Ruiz, S. A., Cañón Barriga, J. E., & Martínez, J. A. (2022). Assessment and validation of wind power potential at convection-permitting resolution for the Caribbean region of Colombia. *Energy* (Oxford, England), 244(123127), 123127. https://doi.org/10.1016/j.energy.2022.123127

Haidekker, M. A. (2020). Stability analysis for linear systems. In *Linear Feedback Controls* (pp. 145–156). Elsevier.

Hirst, L. C. (2012). Principles of solar energy conversion. In *Comprehensive Renewable Energy* (pp. 293–313). Elsevier.

Hosseini Dehshiri, S. S., & Firoozabadi, B. (2023). Comparison, evaluation and prioritization of solar photovoltaic tracking systems using multi criteria decision making methods. *Sustainable Energy Technologies and Assessments,* 55(102989), 102989. https://doi.org/10.1016/j.seta.2022.102989

International Energy Agency. (n.d.). Energy Statistics Data Browser. IEA. Retrieved January 15, 2023, from *https://www.iea.org/data-and-statistics/data-tools/energy-statistics-data-browser?country=COLOMBIA&fuel=Energy%20supply&indicator=TESbySource*

López, A. R., Krumm, A., Schattenhofer, L., Burandt, T., Montoya, F. C., Oberländer, N., & Oei, P.-Y. (2020). Solar PV generation in Colombia - A qualitative and quantitative approach to analyze the potential of solar energy market. *Renewable Energy*, 148, 1266–1279. https://doi.org/10.1016/j.renene.2019.10.066

Mamodiya, U., & Tiwari, N. (2021). Design and implementation of an intelligent single axis automatic solar tracking system. Materials Today: *Proceedings. https://doi.org/10.1016/j.matpr.2021.04.428*

Mauleón, I. (2022). A statistical model to forecast and simulate energy demand in the long-run. *Smart Energy*, 7(100084), 100084. https://doi.org/10.1016/j.segy.2022.100084

Pupo-Roncallo, O., Campillo, J., Ingham, D., Hughes, K., & Pourkashanian, M. (2019). Large scale integration of renewable energy sources (RES) in the future Colombian energy system. *Energy* (Oxford, England), 186(115805), 115805. https://doi.org/10.1016/j.energy.2019.07.135

Ramful, R., & Sowaruth, N. (2022). Low-cost solar tracker to maximize the capture of solar energy in tropical countries. *Energy Reports*, 8, 295–302. https://doi.org/10.1016/j.egyr.2022.10.145

Ros, A. J., & Sai, S. S. (2023). Residential rooftop solar demand in the U.S. and the impact of net energy metering and electricity prices. *Energy Economics*, 118(106491), 106491. https://doi.org/10.1016/j.eneco.2022.106491

Sagastume Gutiérrez, A., Balbis Morejón, M., Cabello Eras, J. J., Cabello Ulloa, M., Rey Martínez, F. J., & Rueda-Bayona, J. G. (2020). Data supporting the forecast of electricity generation capacity from non-conventional renewable energy sources in Colombia. *Data in Brief,* 28(104949), 104949. https://doi.org/10.1016/j.dib.2019.104949

Shapiro, F. R. (2022). The position of the sun based on a simplified model. *Renewable Energy,* 184, 176–181. https://doi.org/10.1016/j.renene.2021.11.084

Zapata, S., Castaneda, M., Aristizabal, A. J., & Dyner, I. (2022). Renewables for supporting supply adequacy in

Colombia. *Energy* (Oxford, England), 239(122157), 122157. https://doi.org/10.1016/j.energy.2021.122157

Zhang, J., Abbasi, K. R., Hussain, K., Akram, S., Alvarado, R., & Almulhim, A. I. (2022). Another perspective towards energy consumption factors in Pakistan: Fresh policy insights from novel methodological framework. *Energy* (Oxford, England), 249(123758), 123758. https://doi.org/10.1016/j.energy.2022.123758

Zhang, Y., Zhang, Y., Zhang, Y., & Zhang, C. (2022). Effect of physical, environmental, and social factors on prediction of building energy consumption for public buildings based on real-world big data. *Energy* (Oxford, England), 261(125286), 125286. https://doi.org/10.1016/j.energy.2022.125286

Zhong, Q., Nelson, J. R., Tong, D., & Grubesic, T. H. (2022). A spatial optimization approach to increase the accuracy of rooftop solar energy assessments. *Applied Energy,* 316(119128), 119128. https://doi.org/10.1016/j.apenergy.2022.119128